Technical Sciences
Academy of Romania
www.jesi.astr.ro

Journal of Engineering Sciences and Innovation
Volume 5, Issue 3 / 2020, p. 197-204

A. Mechanical Engineering

Received ***12 May 2020*** *Accepted* ***15 September 2020***
Received in revised from ***3 August 2020***

Damage detection of critical zones of wind turbine blades based on the complementary methods

PAUL DORU BARSANESCU[1*], NICOLETA IFTIMIE[2], ROZINA STEIGMANN[2], GABRIEL SILVIU DOBRESCU[2], NARCIS ANDREI DANILA[1,2], ADRIANA SAVIN[2]

[1]*Faculty of Mechanical Engineering,*
Gheorghe Asachi Technical University, Iasi, Romania
[2]*Nondestructive Testing Department,*
National Institute of R&D for Technical Physics, Iasi, Romania

Abstract. The wind turbine blades are usually subject to random and complex mechanical stresses. The most common defects in turbine blades may be faulty microscopic and mesoscopic appeared in matrix, not detected by classical nondestructive testing (i.e. using phased array sensors), broken fibers can also appear and develop under moderated loads, or cracks and delaminations due to low energy impacts, etc. The paper presents the results obtained from testing and monitoring of a scalable wind turbine blade (WTB) using different sensors placed on critical location, which were determined by finite element method (FEM) simulation. A comparison between the complementary methods is carried out in order to choose the most efficient method in order to assure the safety in functioning of WTB.

Keywords: nondestructive testing, wind turbine blades, wireless sensors, Fiber Brag Gratings and strain gauges.

1. Introduction

Energy conversion in the frame of climate change and renewable technology development become a priority to secure an energy supply whatever the country is industrialized or on the way for it [1]. As of the end of 2018, the new installed capacity of all wind turbines installed worldwide reached 597GW according to preliminary statistics published by WWEA (World Wind Energy Association). 2018 has been second year in a row, with a higher number of new installations, but

[*]Correspondence address: paulbarsanescu@yahoo.com

with a smaller rate of 9.1% after an increasing of 10.8% in 2017. Thus, al wind turbines installed until the end of 2018 shall cover 6% from the global electric energy requirement. Wind turbines (WTs) are exposed to highly variable and harsh weather conditions, including calm to severe winds, tropical heat, lightning, arctic cold, hail, and snow. Due to these external variations, WTs undergo constantly changing loads, which result in highly variable operational conditions that lead to intense mechanical stress [2,3,4,5].

The structural health monitoring (SHM) system is a process of implementing a damage detection strategy for engineering infrastructure usually related to aerospace, civil and mechanical engineering [6,7]. The active SHM approach for the glass fiber reinforced plastic composite (GFRP) of wind turbine blades (WTBs), addresses the important and complicated problem of signal noise.

Due to its heavy and large structure, it is very difficult to monitor the condition of the turbine components, thus a technique which provides more diagnostics information [8,9,10,11] is required. The SHM condition data could be used as a part of a condition monitoring to minimize the time required for inspection of segments, avoid unnecessary substitution of components and to prevent down time failures [12].

Wireless sensors (WRS) used for SHM applications [13,14,15], includes radio-frequency identification (RFID) technology [16,17]. RFID tag sensors provide identification data and monitor of physical parameters of tagged objects without having an active sensor in the tag circuitry [18,19,20,21,22]. Nowadays, passive, printable, mass deployable, low cost, environmentally RFID tag sensor has been reported for monitoring the sensing parameters. NDT is required both during fabrication and in-service. Starting from the scheme presented in Fig. 1, flaws mentioned above must be detected and evaluated by nondestructive methods with good probability of detection (POD) under high reliability coefficient.

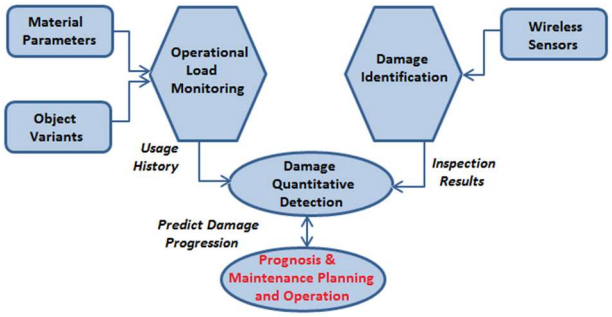

Fig. 1. System Architecture of Structural Health Monitoring (SHM).

Based on the diagnosis and prognosis, the appropriate maintenance strategy can be taken to minimize WT downtime, and improve WT reliability and life-span. The paper presents the results of testing of a scalable WTB, in static conditions, using WRS embedded within in order to monitor possible damages. To determine the righteous of solutions, reliability of correct diagnosis probability, prognosis and

evaluation of residual lifetime and maintenance management, a scalable WTB has been constructed, that had the scaled dynamics of a full scale blade as well as enough sensors for measurements and monitoring. The maximum stress zones and damage evolution and remnant stress [23] have been determined using Finite Element Modelling (FEM). The results of complex mechanical tests performed on scalable WTB (in our case a blade of 1750mm length) are used to give efficiency to monitoring strategy.

2. Principle of methods

The number and location of sensors on WTB may influence the performance of these. The limitation of a small number of measurements zones and under the constraint require that these zones should be selected with *apriori* knowledge of the critical zones.

The blade has been realized from E-glass/epoxy EPIKOTE Resin MGS LR 385 composite. The leading edge is straight and the trailing edge conical for an easy construction. The profile follows NACA airfoil. For increased structural strength and stiffness at 0.286R (R- the total length of distance between the center of rotor and the tip of blade), the same NACA has been applied both for the upper surface and lower surface, keeping the aerodynamically performances of the blade's tip. The profiles between 0.268R and tip were linear interpolated. A compromise has to be found between high-resolution and long propagation distance.

In order to establish the critical zones, FEM was used implying ANSYS Academic version, the maximum dimension of an element was 8 mm, 1338842 nodes and 832563 elements were employed. The FEM model takes into account the presence of the reinforcement structure, which's mass cannot be neglected, especially if one considers that the distance from the axis of rotation increase the inertia and can reduce the frequency associated with the first mode of vibration of WTB. Fig. 2a presents the division of the blade in critical regions. In Fig. 2b is presented the loading forces disposition towards blade axis, a compression force of 500 N has been applied on Y axis (blade upper shell) on a region with 100 mm width. The produced displacement of the tip is of 30.082 mm.

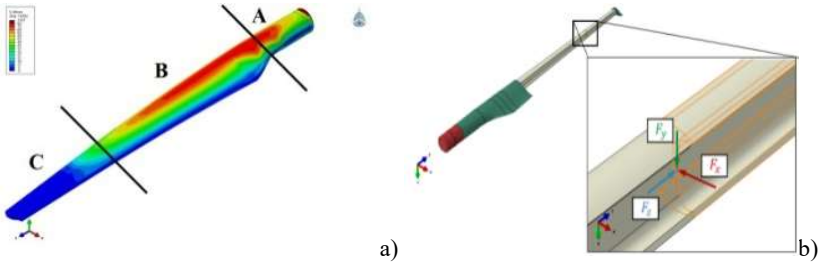

a) b)

Fig. 2. FEM simulation: a) division of blade in critical regions; b) loading forces disposition.

The maximum stresses on WTB appear closely to the joint between the hub and the longeron and at transition between circular geometry to NACA profile.

Three sensors C2A-06-062WW-350, stacked rosette were used, each having 3 strain gauges with 350 Ω electrical resistance were employed (Figs. 3a), connected to Vishay P3 Strain Indicator and recorder, in quarter bridge with automatic balance. Their positioning (Fig. 3b) has allowed the determination of deformations due to bending along blade axis at distance of 488 mm from the fixed end, respectively close to trailing edge at 409mm from the fixed end, as well as closely to the leading edge at 351 mm from the hub. The test were carried out in 7 stages in 100 N steps, maximum of bending of 900.90 Nm.

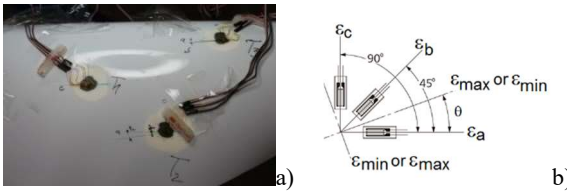

Fig. 3. Strain gauges measurements: a) stress/strain gauge; b) positioning of the stacked gauges.

In order to obtain the best sensor with MM for monitoring the WTB, a sensor which allows the determination of resonance frequency displacement at the changing of dielectric properties from the sample has been developed. The system consist in a RFID reader and a RFID tag (Figure 4), the tag including the sensor and the integrate circuit. When the effort is small, the resonance frequency modifies almost linear in function of effort, meaning that the effort can be determined if the resonance frequency is measured [24] as $f_r = c/4\left(L+\Delta L\right)\sqrt{\varepsilon_r}$ with c speed of light in vacuum, L the length of the copper layer, ε_r the dielectric permittivity of the substrate, ΔL is the additional length who compensate the effect due to thickness, width and dielectric constant of the substrate.

The RFID tag antenna assures that the interrogation frequency shall be equal with the one of RFID tag to obtain perfect matching of impedance between antenna tag and IC chip. The interrogation range is one the important factors for LC passive WRS. The smallest amount of energy must be transmitted toward reader to activate RFID tag, meaning that the transmitted power threshold reach minimum value at resonance frequency. The RFID tag is bonded to the WTB structure subdued to loadings.

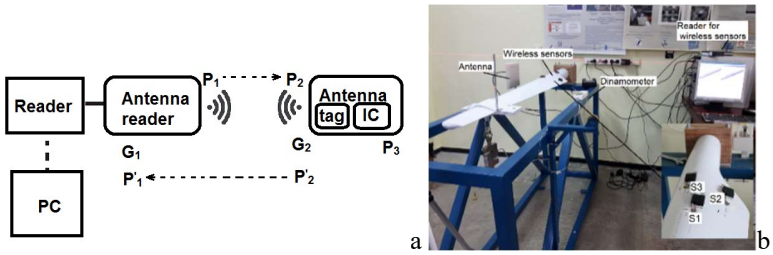

Fig. 4. Wireless sensor system: a) principle; b) experimental set-up.

SHM includes the use of FBG for detecting delamination in composite laminates [25] and monitor impact event occurrence [26,27]. The embedded sensor can monitories the structure in critical regions. The central wavelength of this signal, called Bragg wavelength λB is related to the physical parameters of the grating according to $\lambda_B = 2n\Lambda$ where n is the effective refractive index of the fundamental mode propagating inside the fiber, Λ is the pitch of FBG.

When the fiber containing FBG is submitted to strain, the central wavelength is displaced to higher or smaller values [28]. The direction and the magnitude of displacement is proportional with the modification of strain or temperature. The strain axial sensitivity is $\frac{\partial\lambda_B}{\lambda_B} \approx (1-p_e)\varepsilon$; $\frac{\partial\lambda_B}{\lambda_B} \approx 0.78\varepsilon$, where $\partial\lambda_B$ is the FBG wavelength shift; $\varepsilon << 1$, p_e is photo-elastic coefficient of the fiber $p_e \approx 0.22$, FBG sensors whose gauge lengths are about 10mm were used for SHM. The FBG strain sensing can be expressed as $\varepsilon = \frac{1}{0.78\times10^{-6}}\frac{\Delta\lambda_B}{\lambda_B}$.

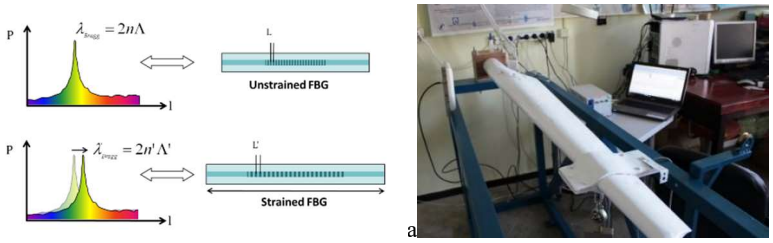

a b

Fig. 5: Fiber Bragg Grating: a) response as function of strain; b) experimental set-up.

3. Experimental results and discussions

For stacked rosette, placed into the critical region indicated by FEM, the sensor denoted T1 measures the deformations of the blade in the plane of I shape longeron, having height/width variable along the blade, T2 measures the deformations of blade shell closely to the trailing edge and T3 measures the deformations of blade shell closely to leading edge. The experimental data were used to calculate [29] maximum strain ε_{max}, minimum strain ε_{min}, acute angle from the axis θ, the maximum shear strain γ_{max}, maximum normal stress σ_{max}, minimal normal stress σ_{min} and maximum shear stress τ_{max}.(Figure 6) The unloading plots are symmetrical with the loading ones.

The reader antenna is fixed at 30 cm from the middle area of WRS placement locus, is connected to a logger reader coupled to PC by USB. IC frequency range is 840 MHz to 960 MHz. The results of bending tests in a loading-unloading cycle are presented in Figs. 7a and b. At 700 N loadings, the maximum deformations are characteristics for sensor S1 (see inlet in Fig. 4b) placed along longeron axis and the minimums are for sensor S2 placed outside the critical zone. In addition, the

deformation is linear, the loading remain in elastic range. During the unloading, the values follow the same characteristic as at loading.

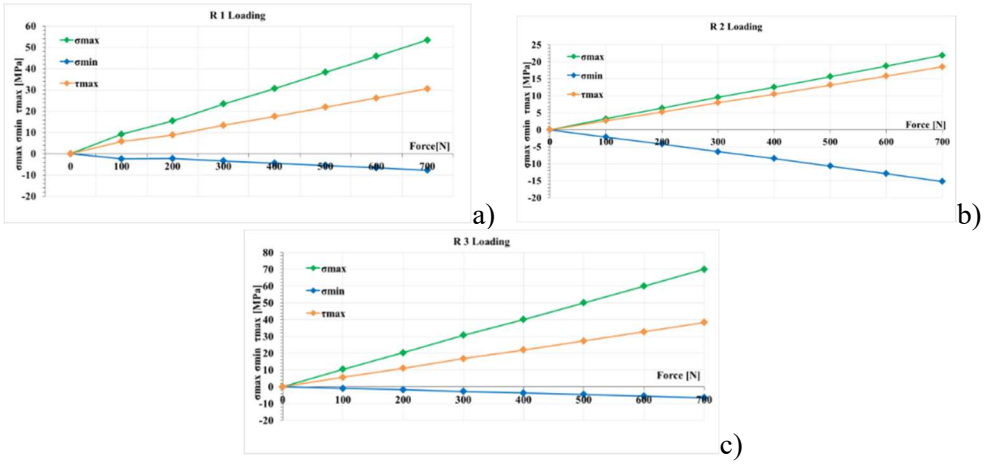

Fig. 6. Variation of stresses with force at loading: a) rosette 1; b) rosette 2; c) rosette 3.

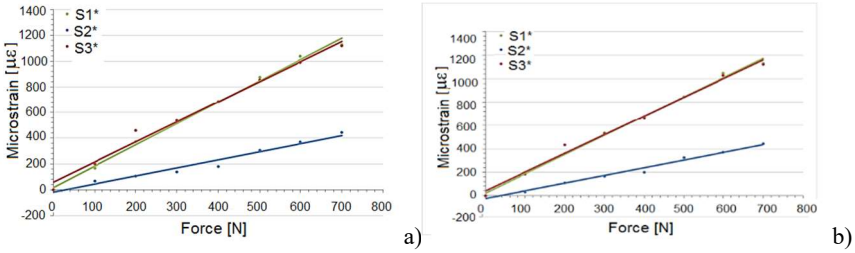

Fig. 7. Signal delivered by the three WRS placed in different critical regions of WTB: a) loading; b) unloading.

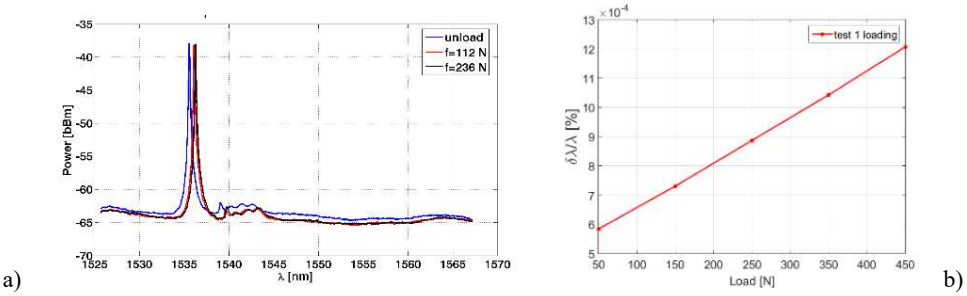

Fig. 8. FBG measurements: a) response to successive loading;
b) relative variation of Bragg wavelength.

Comparing loading/unloading data with the simulated ones, a good correlation of the displacement is found, experimentally being determined as 37 mm.

The OF sensor, FBG single DTG S-01 type used for monitoring have center wavelength in 1535 nm with strain sensitivity $7.8\times10^{-7}\,\mu\varepsilon^{-1}$ and temperature

sensitivity $6.5\times10^{-6}\,\mathrm{K}^{-1}$. This is connected at optical system FS22 Industrial BraggMETER HBM Germany coupled with PC. During the experiments, the temperature has been maintained constant at 22 ± 1°C. The experimental test was performed as applying progressively loading/unloaded forces [30]. Fig. 8a presents the raw data recorded by the device for different loadings. The relative variation of Bragg wavelength was determined in function of loading is presented in Fig. 8b showing that the relative variation of Bragg wavelength is linear.
The same linear dependency strain-load can be shown, even the existence of a remnant stress at force removal, indicating an accumulation of energy in WTB composite structure, preponderant in the resin.

4. Conclusions

Scalable WTB have been constructed and tested to loadings using WRS, OF-FBG and SG located in the maximum concentration stress zones.
The tests were carried on scalable models, in the further research the WRS sensors will be embedded, because in the frame of the project that sustains the paper, the blades will be employed into a demonstrator to show the righteous of solutions, reliability of correct diagnosis probability, prognosis, and evaluation of residual lifetime and maintenance management.

Acknowledgements.
This work was supported by the Romanian Ministry of Research and Innovation, Nucleus Program PN 19 26 01 02 and Project 11 PFE/2018.

References

[1] Fischer K., Besnard F. and Bertling L., *Reliability-centered maintenance for wind turbines based on statistical analysis and practical experience*, IEEE Transactions on Energy Conversion, **27**, 1, 2011, p. 184-195.
[2] McMillan D. and Ault G.W., *Condition monitoring benefit for onshore wind turbines: sensitivity to operational parameters*, IET Renewable Power Generation, **2**, 1, 2008, p. 60-72.
[3] Kawai H., Michishita K. and Deguchi A., *July. Design wind loads on a wind turbine for strong wind*, Proceedings of the BBAA VI International Colloquium on: Bluff Bodies Aerodynamics & Applications, Milano, Italy (Vol. 2024), 2008.
[4] Adams D., White J., Rumsey M. and Farrar C., *Structural health monitoring of wind turbines: method and application to a HAWT*, Wind Energy, **14**, 4, 2011, p. 603-623.
[5] Yang B. and Sun D., *Testing, inspecting and monitoring technologies for wind turbine blades: A survey,* Renewable and Sustainable Energy Reviews, **22**, 2013, p. 515-526.
[6] Joshuva A. and Sugumaran V., *Fault diagnostic methods for wind turbine: A review*, ARPN Journal of Engineering and Applied Sciences, **11**, 7, 2016, p. 4654-4668.
[7] Catbas F.N., *Structural health monitoring: applications and data analysis*, Structural health monitoring of civil infrastructure systems (p. 1-39), Woodhead Publishing, 2009.
[8] Savin A., Steigmann R., Iftimie N., Stanciu M.D., Danila N.A. and Barsanescu P. D., *Integration of complementary methods for monitoring stress/strain of wind turbine blades structures*, MATEC Web of Conferences (Vol. 112, p. 07009), EDP Sciences, 2017.
[9] Balageas D., Fritzen C.P. and Güemes A. eds., *Structural health monitoring* (Vol. 90), John Wiley & Sons, 2010.

[10] Farrar C.R. and Worden K., *An introduction to structural health monitoring*, Philosophical Transactions of the Royal Society A: Mathematical, Physical and Engineering Sciences, **365***,* 1851, 2006, p. 303-315.
[11] Worden K., Farrar C.R., Manson G. and Park G., *The fundamental axioms of structural health monitoring*, Proceedings of the Royal Society A: Mathematical, Physical and Engineering Sciences, **463**, 2082, 2007, p. 1639-1664.
[12] Lynch J.P. , Sundararajan A., Law K.H., Kiremidjian A.S. and Carryer E., *Embedding damage detection algorithms in a wireless sensing unit for operational power efficiency*, Smart Materials and Structures, **13***,* 4, 2004, p. 800.
[13] Lynch J.P., Wang Y., Swartz R.A., Lu K.C. and Loh C.H., *Implementation of a closed-loop structural control system using wireless sensor networks*, Struct. Health Monit., **15**, 4, 2008, p. 518-539.
[14] Lehpamer H., *RFID design principles*. Artech House. Norwood, 2012.
[15] Bolic M., Simplot-Ryl D. and Stojmenovic I. eds., *RFID systems: research trends and challenges*, John Wiley & Sons, 2010.
[16] Chen T., Li S. and Sun H., *Metamaterials application in sensing*, Sensors, **12***,* 3, 2012, p. 2742-2765.
[17] Schueler M., Mandel C., Puentes M. and Jakoby R., *Metamaterial inspired microwave sensors*, IEEE Microwave Magazine, **13**, 2, 2012, p. 57-68.
[18] Tanner N.A., Wait J.R., Farrar C.R. and Sohn H., *Structural health monitoring using modular wireless sensors*, Journal of Intelligent Material Systems and Structures, **14**, 1, 2003, p. 43-56.
[19] Simon T.M., Thomas B.H., Smith R.T. and Smith M., *Adding input controls and sensors to RFID tags to support dynamic tangible user interfaces*, Proceedings of the 8th International Conference on Tangible, Embedded and Embodied Interaction (p. 165-172), ACM, 2014, February.
[20] Smith J.R., Sample A.P., Powledge P. S., Roy S. and Mamishev A., *A wirelessly-powered platform for sensing and computation*, International Conference on Ubiquitous Computing (p. 495-506), Springer, Berlin, Heidelberg, 2006, September.
[21] Lenau T., Ikemoto Y., Suzuki S., Okamoto H., Murakami H., Asama H., Morishita S., Mishima, T., Lin, X. and Itoh, H., *Force sensor system for structural health monitoring using passive RFID tags*, Sensor Review, 2009.
[22] Savin A., Steigmann R., Bruma A. and Šturm R., *An electromagnetic sensor with a metamaterial lens for nondestructive evaluation of composite materials*, Sensors, **15**, 7, 2015, p. 15903-15920.
[23] Ataya S. and Ahmed M.M., *Damages of wind turbine blade trailing edge: Forms, location, and root causes,* Engineering Failure Analysis, **35**, 2013, p. 480-488.
[24] Savin A., Iftimie N., Steigmann R., Rosu D., Dobrescu G.S., Grum J. and Barsanescu P. D., *Effective Methods for Structural Health Monitoring of Critical Zones of Scalable Wind Turbine Blades*, Strojniski Vestnik/Journal of Mechanical Engineering, **64**, 11, 2018.
[25] Takeda S.I., Aoki Y. and Nagao Y., *Damage monitoring of CFRP stiffened panels under compressive load using FBG sensors*. Composite Structures, **94**, 3, 2012, p. 813-819.
[26] Kuang K., Kenny R., Whelan M.P., Cantwell W.J. and Chalker P. R., *Embedded fibre Bragg grating sensors in advanced composite materials*, Composites Science and Technology, **61**, 10, 2001, p. 1379-1387.
[27] López-Higuera J.M. ed., *Handbook of Optical Fibre Sensing Technology*, Wiley and Sons: Chichester, West Sussex, UK, 2002.
[28] Gouveia C.A., Baptista J.M. and Jorge P. A., *Refractometric optical fiber platforms for label free sensing*, Current Developments in Optical Fiber Technology, IntechOpen, 2013.
[29] Sciammarella CA and Sciammarella FM, *Strain gage rosettes: selection, application and data reduction Experimental Mechanics of Solids*, John Wiley & Sons Ltd, 2012, p. 111-121
[30] ASTM D5868 - 01(2014). Standard Test Method for Lap Shear Adhesion for Fiber Reinforced Plastic (FRP) Bonding, ASTM International, West Conshohocken, 2014.